

Effect of Deep-Stall Wing Dynamics on Forebody-Induced Wing Rock

Lars E. Ericsson*
Mt. View, California 94040

Introduction

A RECENT review¹ of wing rock of advanced aircraft, such as X-29A, X-31, and F-18 HARV, showed that wing rock occurs first at moderate angles of attack² through dynamic stall³ of outer wing panels with moderately swept leading edges. This is illustrated by the experimental results for the X-29A aircraft⁴ (Fig. 1). When this type of wing rock was suppressed by the use of the flaperons, forebody-induced wing rock occurred at higher angles of attack, $\alpha > 35$ deg (Fig. 1b). The driving flow mechanism for the wing rock at these high angles of attack is the moving wall effect⁵ on the forebody crossflow separation at $\alpha > \theta_A$, where θ_A is the forebody apex half-angle.⁶ The wing rock reaches its maximum amplitude at an angle of attack just below that for which static asymmetric crossflow separation occurs,⁷ i.e., at $\alpha < 2\theta_A$ (Ref. 6). At $\alpha > 2\theta_A$, the moving wall effect has to overcome the static crossflow asymmetry. This is the reason for the rapid decrease of the limit cycle amplitude for $\alpha > 55$ deg in Fig. 1b. In the analysis in Ref. 1 of the experimentally observed wing rock of a generic aircraft model⁸ (Fig. 2), a certain roll-damping value had to be assumed to obtain a limit-cycle oscillation. In the wind-tunnel test⁸ bearing friction could have supplied the needed roll damping. However, in free flight, the roll damping has to be generated by other means to obtain an oscillation of the limit-cycle type. As discussed in Ref. 1, the only source of this roll damping at high angles of attack is the deep-stall damping-in-plunge of the outboard wing sections.

The wing on the generic aircraft model⁸ (Fig. 2) has a flat-plate airfoil section. It and the inverted 7.4% Clark Y airfoil have very similar deep-stall $c_l(\alpha)$ characteristics⁹ (Fig. 3). Judging by the deep-stall characteristics for the NACA 0012 and NACA 0015 airfoil sections¹⁰ (Fig. 4), the mean $c_l(\alpha)$ slope at $\alpha > 8$ deg in Fig. 3 should give a conservative estimate for the flat-plate airfoil section, i.e., $c_{l\alpha} \approx 0.95$. As the tangential force is negligibly small, $c_{m\alpha} \approx 0.95/\cos \alpha$. For the plunging wing section during wing rock, the sectional normal force at the spanwise location $y = \eta b/2$, where b is the wing span, is

$$c_n(\eta) = c_{m\alpha} \dot{z}/U_\infty \quad (1)$$

where \dot{z} is the plunging velocity of the wing section.

For $(\dot{z}/U_\infty)^2 \ll 1$ and $\phi^2 \ll 1$, where ϕ is the roll angle, one obtains

$$\dot{z}/U_\infty = (b\dot{\phi}/2U_\infty)\eta \cos \sigma \quad (2)$$

where σ is the inclination of the roll axis.

Thus, the roll-rate-induced normal force coefficient on the spanwise extent $dy = (b/2) d\eta$ is

$$\Delta c_n = c_{m\alpha}(\eta) \left(\frac{b\dot{\phi}}{2U_\infty} \right) \eta \cos \sigma c(\eta) \left(\frac{b}{2} \right) \frac{d\eta}{S} \quad (3)$$

Presented as Paper 96-3404 at the AIAA Atmospheric Flight Mechanics Conference, San Diego, CA, July 29–31, 1996; received Aug. 11, 1996; revision received Jan. 27, 1997; accepted for publication Jan. 27, 1997. Copyright © 1997 by L. E. Ericsson. Published by the American Institute of Aeronautics and Astronautics, Inc., with permission.

*Engineering Consultant. Fellow AIAA.

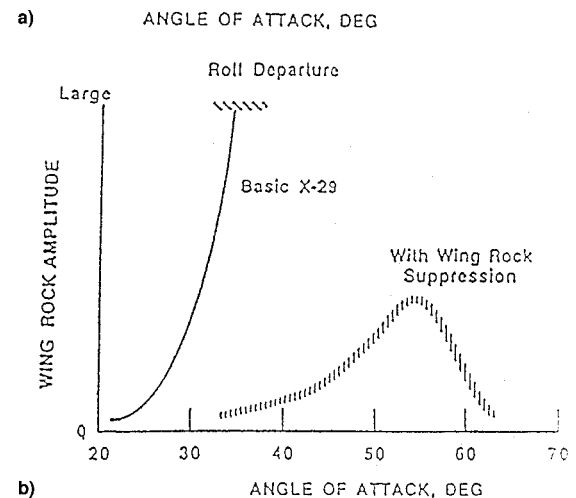
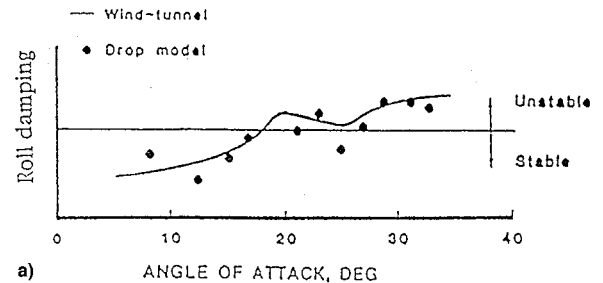
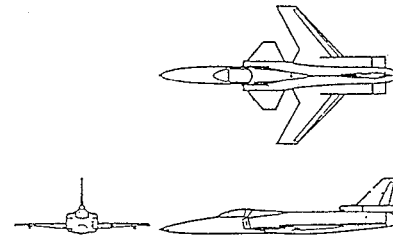


Fig. 1 Wing rock of the X-29A aircraft⁴: a) roll damping of X-29A models and b) wing rock characteristics of the X-29A aircraft.

where S is the wing reference area and $c(\eta)$ is the local stream-wise wing chord. Equation (3) gives

$$\Delta c_{n\dot{\phi}} = \frac{\partial(\Delta c_n)}{\partial(b\dot{\phi}/2U_\infty)} = c_{m\alpha}(\eta) \cos \sigma c(\eta) \left(\frac{b}{2S} \right) \eta d\eta \quad (4)$$

For a tapered wing with tip chord c_t , straight trailing edge, and leading-edge sweep Λ_{LE} , i.e., the wing geometry of the generic aircraft model⁸ in Fig. 2, one obtains

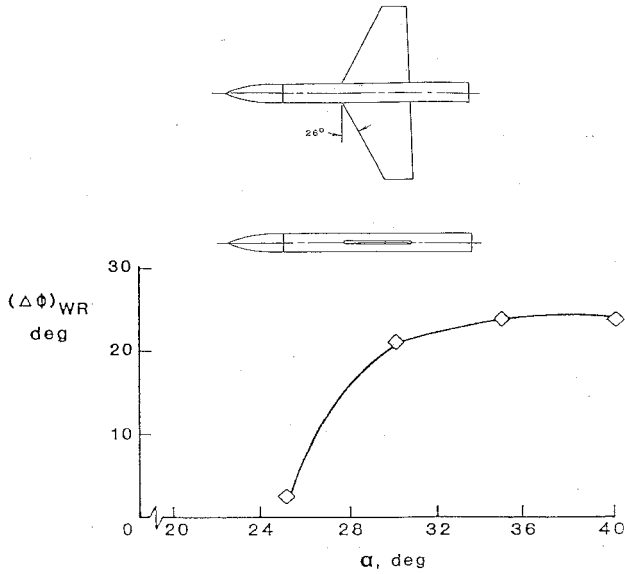
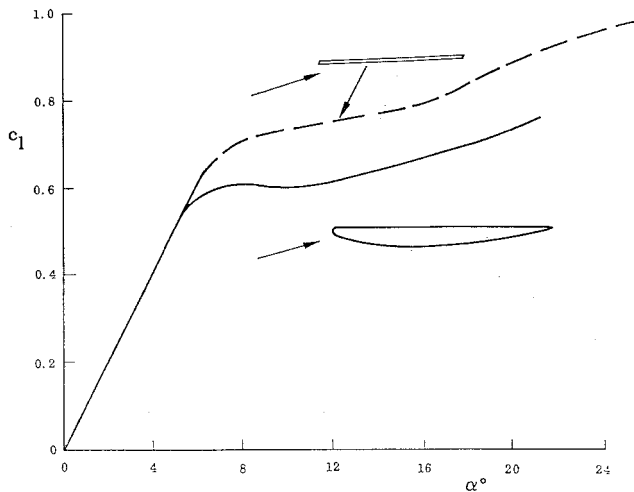
$$c(\eta) = c_t + (b/2)(1 - \eta) \tan \Lambda_{LE} \quad (5)$$

Assuming that the load distribution is elliptic (at constant angle of attack along the span), one obtains

$$c_{m\alpha}(\eta) = c_{m\alpha}(0)(1 - \eta^2)^{1/2} \quad (6)$$

The contribution to the roll-damping derivative is

$$\Delta c_{n\dot{\phi}} = -\Delta c_{n\dot{\phi}}(b/2)\eta/b \quad (7)$$

Fig. 2 Wing rock of generic aircraft configuration.⁸Fig. 3 $c_l(\alpha)$ characteristics for inverted 7.4% Clark Y and flat-plate airfoils.⁹

Combining Eqs. (4-7) gives the following expression for the roll-damping derivative:

$$c_{l\dot{\phi}} = - \int_0^1 \Delta c_n \dot{\phi} \frac{\eta}{2} = - \int_0^1 c_{m\eta}(\eta) \cos \sigma c(\eta) \left(\frac{b}{2S} \right) \eta^2 d\eta$$

$$= - \left(\frac{b^2}{2S} \right) c_{m\eta}(0) \cos \sigma \left[\left(\frac{\pi c_t}{16b} \right) + \left(\frac{\pi}{32} - \frac{1}{15} \right) \tan \Lambda_{LE} \right] \quad (8)$$

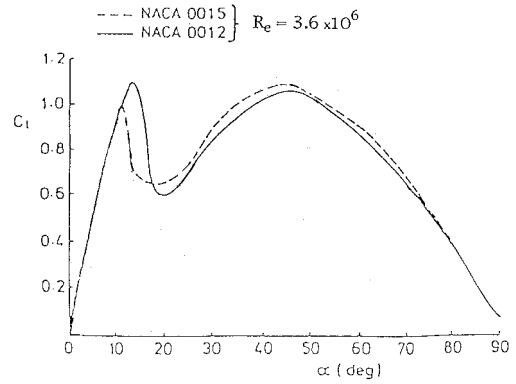
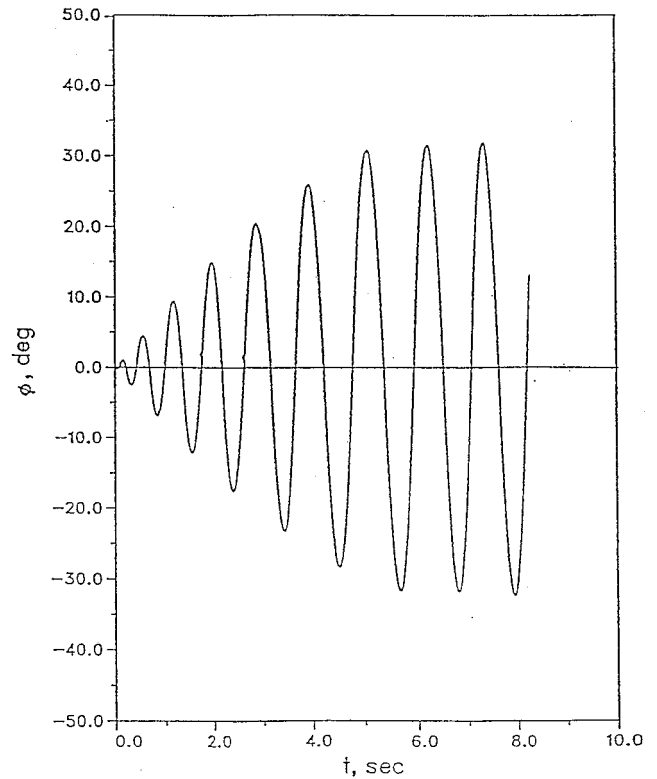
For a straight wing, where $\Lambda_{LE} = 0$ and $c_t = c$, Eq. (8) gives

$$c_{l\dot{\phi}} = -(\pi/32)c_{m\eta}(0)\cos \sigma \quad (9)$$

For the generic aircraft model⁸ (Fig. 2), where $\Lambda_{LE} = 26$ deg, $b^2/S = 0.336$, and $c_t/b = 0.116$, Eq. (8) gives

$$c_{l\dot{\phi}} = -0.022c_{m\eta}(0)\cos \sigma \quad (10)$$

In the computation¹ producing the results shown in Fig. 5, $c_{l\dot{\phi}} = -0.018$ was assumed, giving a limit-cycle amplitude of 32 deg. The measured amplitude⁸ for the circular cross section (Fig. 2) is 24 deg at $\alpha = 35$ deg, not 32 deg. According to

Fig. 4 $c_l(\alpha)$ characteristics from $\alpha = 0$ to 90 deg for NACA 0012 and NACA 0015 airfoils.¹⁰Fig. 5 Computed wing rock time history at $\alpha = 35$ deg.¹

an earlier discussion, $c_{m\eta}(0) = 0.95/\cos \sigma$, which in Eq. (10) gives $c_{l\dot{\phi}} = -0.021$. Using this value rather than $c_{l\dot{\phi}} = -0.018$ would have resulted in a predicted limit-cycle amplitude of 27 deg rather than 32 deg (Fig. 5). The remaining difference could probably be accounted for by the ball-bearing friction present in the wind-tunnel test.⁸ The results in Fig. 4 show that for a flight vehicle with a NACA airfoil wing section the deep-stall $c_l(\alpha)$ slope would be much larger than 0.95, resulting in a predicted limit-cycle amplitude substantially lower than 27 deg.

Conclusions

A simple one degree-of-freedom analysis has demonstrated that the limit-cycle roll oscillation observed in wind-tunnel tests of a generic aircraft model will also occur in free flight, in which case the roll damping needed to establish the limit-cycle type of oscillation is provided by the deep-stall damping-in-plunge of the streamwise wing sections, without any assistance from the frictional type of damping present in wind-tunnel tests.

Acknowledgments

This paper is, in part, based upon results obtained in a study performed for ARPA, Contract DAAH01-94-C-R022, under the direction of M. S. Francis.

References

- ¹Ericsson, L. E., Mendenhall, M. R., and Perkins, S. C., Jr., "Review of Forebody-Induced Wing Rock," *Journal of Aircraft*, Vol. 33, No. 2, 1996, pp. 253–259.
- ²Ericsson, L. E., "Various Sources of Wing Rock," *Journal of Aircraft*, Vol. 27, No. 6, 1990, pp. 488–494.
- ³Ericsson, L. E., and Reding, J. P., "Fluid Dynamics of Dynamic Stall, Part I, Unsteady Flow Concepts," *Journal of Fluids and Structures*, Vol. 2, Jan. 1988, pp. 1–33.
- ⁴Fratello, D. J., Croom, M. A., Nguyen, L. T., and Domack, C. S., "Use of the Updated NASA Langley Radio-Controlled Drop-Model Technique for High-Alpha Studies of the X-29A Configuration," AIAA Paper 87-2559, Aug. 1987.
- ⁵Ericsson, L. E., "Moving Wall Effects in Unsteady Flow," *Journal of Aircraft*, Vol. 25, No. 11, 1988, pp. 977–990.
- ⁶Ericsson, L. E., and Reding, J. P., "Asymmetric Flow Separation and Vortex Shedding on Bodies of Revolution," *Tactical Missile Aerodynamics: General Topics*, edited by M. J. Hemsch, Vol. 141, Progress in Astronautics and Aeronautics, AIAA, Washington, DC, 1992, pp. 391–452.
- ⁷Ericsson, L. E., "Unsteady Separation on Slender Bodies at High Angles of Attack," *Journal of Spacecraft and Rockets*, Vol. 30, No. 6, 1993, pp. 689–695.
- ⁸Brandon, J. M., and Nguyen, L. T., "Experimental Study of Effects of Forebody Geometry on High Angle of Attack Stability," *Journal of Aircraft*, Vol. 25, No. 7, 1988, pp. 591–597.
- ⁹Bollay, W., and Brown, C. D., "Some Experimental Results on Wing Flutter," *Journal of the Aeronautical Sciences*, Vol. 8, No. 6, 1941, pp. 313–318.
- ¹⁰Raghunathan, S., Harrison, J. R., and Hawkins, B. D., "Thick Airfoil at Low Reynolds Numbers and High Incidence," *Journal of Aircraft*, Vol. 25, No. 7, 1988, pp. 669–671.

Prediction of Delta Wing Leading-Edge Vortex Circulation and Lift-Curve Slope

Lance W. Traub*
Texas A&M University,
College Station, Texas 77843-3141

Nomenclature

b	= wing span
C_T	= leading-edge thrust coefficient
c	= chord
c_s	= sectional leading-edge suction coefficient
c_t	= sectional leading-edge thrust coefficient
k_p	= potential constant
q	= dynamic pressure
S	= wing area
t	= sectional leading-edge thrust
U_∞	= freestream velocity
w	= downwash velocity
x	= chordwise direction
y	= spanwise direction

α	= angle of attack
Γ	= vortex circulation
γ	= vorticity per unit length
ε	= wing apex half-angle
Λ	= leading-edge sweep angle
ρ	= density

Subscripts

L.E.	= leading edge
v	= vortex

Introduction

THE leading-edge suction analogy of Polhamus¹ provides an accurate means by which the aerodynamics of slender sharp wings may be estimated. Slender swept wings typically have flowfields dominated by conical leading-edge vortices. The basic tenet of the suction analogy is that the leading-edge suction force through enforced leading-edge flow separation, in combination with sweep, is effectively rotated through 90 deg to the plane of the normal force, and manifests as the force required to effectively maintain equilibrium of the vortex above the wing. The analogy does not, however, yield information on the leading-edge suction distribution or vortex characteristics.

Use of a panel method allows determination of the leading-edge thrust or suction distribution by using the computed attached flow sectional lift and vortex drag at each spanwise station. The leading-edge suction distribution may also be determined analytically, using an expression derived by Purvis² for arbitrary planforms. To calculate the strength of the leading-edge vortex, a panel method may be employed, with various methodologies being used to estimate the vortex strength,³ e.g., calculating the velocity above and below the leading-edge wake. Euler and Navier–Stokes solvers can also be used to determine the vortex properties, but are computationally expensive and sensitive to the grid employed.⁴ None of these computational methods, however, show explicitly the functional relationship of vortex strength to parameters such as wing leading-edge sweep, α , and chordwise location.

Helmholtz' vortex theorems ensure that the rate of change of the spanwise load distribution relates to the rate at which vorticity is shed from a wing's trailing edge ($\gamma = -d\Gamma/dy$). Thus, it may be analogous to assume that the rate of change of the leading-edge thrust distribution relates to the rate at which vorticity is shed from the leading edge, and consequently, into the leading-edge vortex. Using this analogy, combined with the aforementioned expression of Purvis² for the leading-edge suction distribution, allows the derivation of an expression to estimate the leading-edge vortex chordwise circulation distribution. In this Note, an expression is derived to estimate the strength of the leading-edge vortex of delta wings. The vorticity shed from the wing leading edge is related to the rate of change of the wing leading-edge thrust, yielding an expression for γ , which can be integrated to yield vortex circulation. The form of this expression allows derivation of two equations for the potential constant or attached flow lift–curve slope of delta wings.

Hemsch and Luckring⁵ have derived an expression using a Sychev similarity parameter to estimate the strength of the leading-edge vortex at the wing trailing edge. Using this expression it is possible to estimate the strength of the vortex along the wing. This does, however, require the assumption of conical flow (i.e., $\Gamma \propto x$), and two empirical constants.

Discussion of Method

Using the Kutta–Joukowski theorem to calculate the leading-edge thrust associated with the freestream parallel to the chord gives

$$dt = \rho(U_\infty \sin \alpha - w) \frac{d\Gamma}{dy} dy \quad (1)$$

Received Nov. 17, 1996; revision received Feb. 14, 1997; accepted for publication Feb. 14, 1997. Copyright © 1997 by L. W. Traub. Published by the American Institute of Aeronautics and Astronautics, Inc., with permission.

*Graduate Student, Aerospace Engineering Department. Associate Member AIAA.